Double Phase Estimator: a New Unambiguous BOC Tracking Algorithm

Daniele Borio[1], *Member, IEEE*

Abstract

Several new Global Navigation Satellite System (GNSS) modulations adopt a Binary Offset Carrier (BOC) subcarrier to shape the signal spectrum, increase frequency separation and improve tracking performance. BOC modulated signals are however characterized by ambiguous multi-peaked correlation functions and several techniques have been proposed in the literature to solve the problem of locking into secondary peaks. In this paper, a novel unambiguous BOC tracking technique, the Double Phase Estimator (DPE), is designed to account for the effect of signal bandlimiting. The DPE is an effective alternative to the Double Estimator (DE) tracking technique where the Subcarrier Lock Loop (SLL) is replaced by a Subcarrier Phase Lock Loop (SPLL). In the presence of signal bandlimiting, the DPE is able to generate local signal replicas better matched to the input components outperforming the DE. The performance of the DPE is thoroughly characterized and processing of real wide-band BOC signals is used to demonstrate the effectiveness of the algorithm proposed. In addition to this, the DPE requires a lower computational load than the DE and thus should be adopted for the processing of wide-band BOC signals.

Index Terms

BOC Signal, Double Estimator, GNSS, SLL, Tracking.

I. INTRODUCTION

With the advent of new Global Navigation Satellite Systems (GNSSs) such as the European Galileo, the Russian GLONASS and the Chinese Beidou, and the modernization of the US Global Positioning System (GPS), frequency bands allocated for satellite navigation are becoming

1) Institute for the Protection and Security of Citizen (IPSC), Joint Research Centre (ISPRA), Italy. Email: daniele.borio@ieee.org

more and more crowded with a multitude of signals which could create inter- and intra-system interference [1], [2]. In order to improve Radio-Frequency (RF) compatibility among different GNSS signals, new modulations have been introduced [3], [4]. In particular, the Binary Offset Carrier (BOC) modulation [3] allows the signal power to be moved away from its centre frequency reducing frequency overlap with legacy GPS signals which use a Binary Phase Shift Keying (BPSK) modulation. BPSK signals have a power spectrum concentrated around the centre frequency whereas the BOC modulation uses and additional signal component, called subcarrier, to obtain a symmetric spectrum with two main lobes displaced with respect to the centre frequency by $\pm f_{sb}$, the subcarrier repetition frequency. The subcarrier presence significantly reduces interference issues and leads to signals with sharp autocorrelation functions, i.e. with improved ranging capabilities. Despite their improved performance, BOC signals are characterized by multi-peaked correlation functions and secondary peak lock can occur. In particular, GNSS receivers estimate the signal travel time by measuring the relative delay between received and locally generated signals. In turn, the relative delay is obtained by tracking the peak of the signal correlation function and biases can be introduced if a secondary peak is locked. In order to avoid secondary peak lock, several tracking techniques have been designed including Bump-Jump (BJ) [5], Autocorrelation Side-Peak Cancellation Technique (ASPeCT) [6] and its extensions [7], Double Estimator (DE) [8], [9], local sub-carrier shaping [10], side band processing [11] and SubCarrier Cancellation (SCC) [12], [13]. A review of different unambiguous BOC tracking techniques can be found in [14], [15].

Among the different techniques proposed in the literature, the DE has improved performance [8], [9], [14], [16] and a reduced computational load. In particular, DE is able to achieve the performance of standard tracking loops when locked on the main correlation peak. Secondary peak lock is avoided without introducing additional noise. DE exploits the fact that a BOC modulated signal can be represented as the product of a spreading code and the periodic repetition of the subcarrier: the DE tracks their delays independently using two separate tracking loops, the Delay Lock Loop (DLL) for the code and the Subcarrier Lock Loop (SLL) for the subcarrier. When tracked separately, no ambiguity is present and lock on secondary peaks is avoided.

Although the DE recombines delay estimates from DLL and SLL, the usage of separate loops suggests the idea that the subcarrier should be considered similarly to the signal code and carrier and not as a nuisance component causing ambiguity in the correlation function. The

subcarrier can be considered as the source of a new type of measurements, the subcarrier phase. Note that this concept, although often not clearly stated, is implicitly present in the recent GNSS literature. For example, [15] suggested the usage of the LAMBDA methods for solving the BOC ambiguity problem. Several ambiguous subcarrier phase measurements are combined and used similarly as carrier phase observations. Palestini discusses in [17] the combination of delay and subcarrier measurements using a sort of Hatch filter. The possibility of generating subcarrier measurements is precluded in tracking methods which remove or ignore the subcarrier presence [5]–[7], [10], [13]. In addition to this, the subcarrier has characteristics intermediate between code and carrier and thus can be processed using techniques originally designed for these two components. The SLL introduced by [8], [9] operates in the same way as a standard DLL: three complex correlators, namely Early, Prompt and Late, are required and the same DLL discriminators are used. Also [18], which suggested a modification of the DE through the approximation of the subcarrier as a pure sinusoid, uses the same SLL introduced in [8], [9] and treats the subcarrier similarly to the code component. Note that the approximation of the subcarrier as a pure sinusoid was already considered in [12], [13] for the SCC technique. In this case, however the subcarrier component is removed through non-linear processing and the advantages introduced by the subcarrier are lost.

In this paper, the approximation of the subcarrier as a pure sinusoids is further exploited and a new DE architecture is obtained. In particular, the SLL is replaced by a Phase Lock Loop (PLL), the Subcarrier PLL (SPLL), which is used to track the subcarrier phase. In this way, the subcarrier is treated as a carrier component and a new type of loop is introduced. The approximation of the subcarrier as a pure sinusoid is justified by the filtering operated by the receiver front-end. Moreover, some wide-band signals such as the cosine BOC(15, 2.5) adopted by the Galileo Public Regulated Service (PRS) are inherently bandlimited at the transmitter side. In this case, the subcarrier can be better approximated as a pure sinusoid. The architecture proposed is named Double Phase Estimator (DPE) and outperforms the DE in the presence of bandlimited signals. In addition to this, the DPE can be implemented using only an additional correlator with respect to the standard architecture adopted for BPSK signal processing. The DE requires two additional complex correlators and thus is more computationally demanding than the newly proposed solution. The DPE also differs from the solutions suggested by [18] which requires two additional complex correlators and uses a standard SLL.

The performance of the DPE is thoroughly analyzed and the loss caused by approximating the subcarrier as a pure sinusoid is determined. It is shown that even when the subcarrier of the received signal is a perfect square wave, i.e. in the absence of front-end filtering, the maximum loss experienced is -0.91 dB in terms of post-coherent Signal-to-Noise Ratio (SNR). In the presence of front-end filtering, the DPE outperforms other techniques providing a better approximation of the filter matched to the input signal. The tracking jitter [19] of the SPLL is theoretically analyzed and compared with the performance of the DE and SCC technique showing the advantages brought by the DPE. Semi-analytic simulations are used to support the validity of the theory developed.

Finally, the effectiveness of the technique proposed is demonstrated processing real sine BOC(1, 1) and cosine BOC(15, 2.5) signals collected from the Galileo In-Orbit Validation Element (GIOVE)-B satellite. The experimental results further support the theoretical findings and show the effectiveness of the DPE which clearly outperforms the DE for the processing of cosine BOC(15, 2.5) signals.

The remainder of this paper is organized as follows. The model adopted for BOC modulated signals is provided in Section II and the newly proposed DPE is described in Section III. The performance of the DPE is analyzed in Section IV whereas Section V discusses the results obtained by processing real BOC modulated signals. Conclusions are finally drawn in Section VI.

II. SIGNAL AND SYSTEM MODELS

New GNSS signals adopt a subcarrier to shape the signal spectrum, increase frequency separation between different signals and improve tracking performance. When the subcarrier is present, the signal at the input of a GNSS receiver in a one-path additive Gaussian channel can be modeled as

$$y(t) = \sqrt{2C} d\left(t - \tau_0\right) c\left(t - \tau_0\right) s_b\left(t - \tau_0\right) \cos\left(2\pi(f_{RF} + f_0)t + \varphi_0\right) + \eta(t) \qquad (1)$$

where

- C is the power recovered by the receiver;
- $d(\cdot)$ is the navigation message;

- $c(\cdot)$ is a pseudo-random sequence extracted from a family of quasi-orthogonal codes modulated using rectangular pulses. $c(\cdot)$ is used for spreading the signal spectrum;
- $s_b(\cdot)$ is the subcarrier component obtained by periodically repeating a basic waveform of limited duration;
- τ_0, f_0 and φ_0 are the delay, Doppler frequency and phase introduced by the communication channel;
- f_{RF} is the centre frequency of the GNSS signal;
- $\eta(t)$ is a zero-mean Gaussian noise process.

In (1), the impact of the Doppler shift on the code and subcarrier are neglected. The Doppler shift introduces code and subcarrier delay rates that are however recovered by the tracking loops used to estimate the signal parameters. Code and subcarrier delay rates are neglected in (1) to avoid obscuring mathematical details. Finally, note that a GNSS receiver usually recovers several signals from different satellites. However, each signal is characterized by a specific code and the receiver is able to process each signal independently, exploiting the quasi-orthogonality of the codes. For this reason, a single useful component is considered in (1).

Signal (1) is filtered and down-converted by the receiver front-end before being digitized. In the following, the effects of quantization are neglected and it is assumed that the signal is sampled without introducing significant distortions. After down-conversion and sampling, (1) becomes:

$$y[n] = \sqrt{C}\tilde{d}\left(nT_s - \tau_0\right)\tilde{c}\left(nT_s - \tau_0\right)\tilde{s}_b\left(nT_s - \tau_0\right)\exp\left\{j2\pi f_0 nT_s + j\varphi_0\right\} + \eta_{BB}[n] \quad (2)$$

where the notation $x[n]$ is used to denote a discrete time sequence sampled at the frequency $f_s = \frac{1}{T_s}$. The index "BB" is used to denote a signal down-converted to base-band and the symbol $\tilde{\cdot}$ is used to indicate the impact of the front-end filter on the useful signal components.

The noise term, $\eta_{BB}[n]$, is assumed to be a complex Additive White Gaussian Noise (AWGN) with independent and identically distributed (i.i.d.) real and imaginary parts with variance σ^2. This variance depends on the filtering, down-conversion and sampling strategy applied by the receiver front-end and is given by $\sigma^2 = N_0 B_{Rx}$, where B_{Rx} is the front-end one-sided bandwidth and N_0 is the Power Spectral Density (PSD) of the input noise, $\eta(t)$.

Note that front-end filtering may introduce correlation among noise samples. In this case, the hypothesis of a white input noise sequence is not strictly valid and correlation among noise samples should be accounted for [20], [21]. The front-end bandwidth, B_{Rx}, is however much

wider than that of the correlator blocks used to process the input signal. The correlation among noise sample can thus be neglected and the AWGN hypothesis adopted. The ratio between the carrier power, C, and the noise power spectral density, N_0, defines the Carrier-to-Noise density power ratio (C/N_0), one of the main signal quality indicators used in GNSS.

III. DOUBLE PHASE ESTIMATOR

In standard GNSS receivers [22], [23], two tracking loops are used for tracking the variations of the signal parameters, τ_0, f_0 and φ_0. In particular, a DLL is used to track delay variations whereas a PLL is employed to continuously estimate the signal phase and frequency. The DLL operates on both subcarrier and code components, whereas the PLL operates on the carrier. Since subcarrier and code are jointly processed by a standard DLL, locks on secondary peaks of the BOC autocorrelation function can occur. The solution introduced by the DE is to consider the subcarrier and code components independently. More specifically, it is assumed that the two components are affected by different delays and two independent loops are used to track the variations of these two parameters. Estimates provided by the two loops are then recombined to determine the common signal delay. The subcarrier delay is tracked using an SLL that operates in a similar way as a standard DLL: after code and carrier removal, early and late replicas of the subcarrier component are correlated with the incoming signal and used to determine an estimate of the subcarrier autocorrelation gradient. The loop maximizes the subcarrier correlation function by following the gradient direction. A standard DLL is used to maintain lock on the code component that after subcarrier removal reduces to a BPSK signal. The DE removes secondary peaks by projecting the signal correlation function into a two dimensional space where ambiguities are not present [8], [9]. The SLL requires two additional correlators and operates assuming a perfect subcarrier representation, i.e., the subcarrier is not affected by front-end filtering and it is modeled as a perfect square wave. The subcarrier is treated similarly to the code and the SLL exploits the same operating principle of the DLL. In this paper, the subcarrier approximation introduced by [12], [18] is justified in terms of front-end filtering and a solution alternative to the use of the SLL is proposed.

The subcarrier, $s_b(t)$, is a periodic signal with period equal to the code chip duration, T_{ch}. A chip is defined here as the basic element of the pseudo-random sequence, $c(\cdot)$ which assumes a

constant value over the chip duration. For example, a period of the sine BOC is defined as [3], [4]

$$s_b(t) = \text{sign}\left[\sin(2\pi m f_r t)\right] \tag{3}$$

where $f_r = 1.023$ MHz is a reference frequency. Waveform (3) repeats periodically every chip duration, $T_{ch} = \frac{1}{nf_r}$. In this case, m and n are design parameters which define the spectral and temporal characteristics of the BOC subcarrier. If the ratio $\frac{m}{n}$ is an integer, the subcarrier period reduces to $T_{sb} = \frac{1}{f_{sb}} = \frac{1}{mf_r}$. When a cosine BOC is considered, the sine in (3) is replaced by a cosine function and similar considerations apply.

Since $s_b(t)$ is periodic, it can be expanded in Fourier series:

$$s_b(t) = \sum_{i=1}^{+\infty} s_i \sin\left(2\pi i f_{sb} t\right) \tag{4}$$

where s_i are the coefficients of the Fourier series expansion and $f_{sb} = m f_r$ (in the following only the case where m is a multiple of n is considered). In the following, the case of a sine-phased subcarrier is considered. Results for cosine-phased subcarriers can be obtained by writing expansion (4) in terms of cosine functions. Note that $s_b(t)$ is a zero mean signal and the Direct Current (DC) term in (4) is not present.

The signal transmitted by a GNSS satellite is usually bandlimited. Moreover, the filter of the receiver front-end removes high frequency signal components. For this reason, only the lower order terms in (4) are preserved and the filtered subcarrier can be approximated as

$$\tilde{s}_b(t) = \sum_{i=1}^{N_b} s_i \sin\left(2\pi i f_{sb} t\right) \tag{5}$$

where N_b is the number of terms preserved by the front-end filter. If a single term is retained then $\tilde{s}_b(t)$ can be approximated by a single sine wave

$$\tilde{s}_b(t) \approx \tilde{s}_{b,1}(t) = s_1 \sin\left(2\pi f_{sb} t\right) \tag{6}$$

where subscript '1' is used to indicate that only the first term is retained in the series expansion. When the subcarrier is approximated as (6), it can be tracked using an additional PLL instead of the SLL introduced by [8], [9]. A schematic representation of the DPE is provided in Fig. 1. The code component is tracked using a standard DLL whereas the subcarrier delay is recovered using an additional PLL. The symbols $F_c(z)$ and $F_{sb}(z)$ in Fig. 1 denote the transfer functions of the loop filters adopted for the processing of the delay and subcarrier components, respectively.
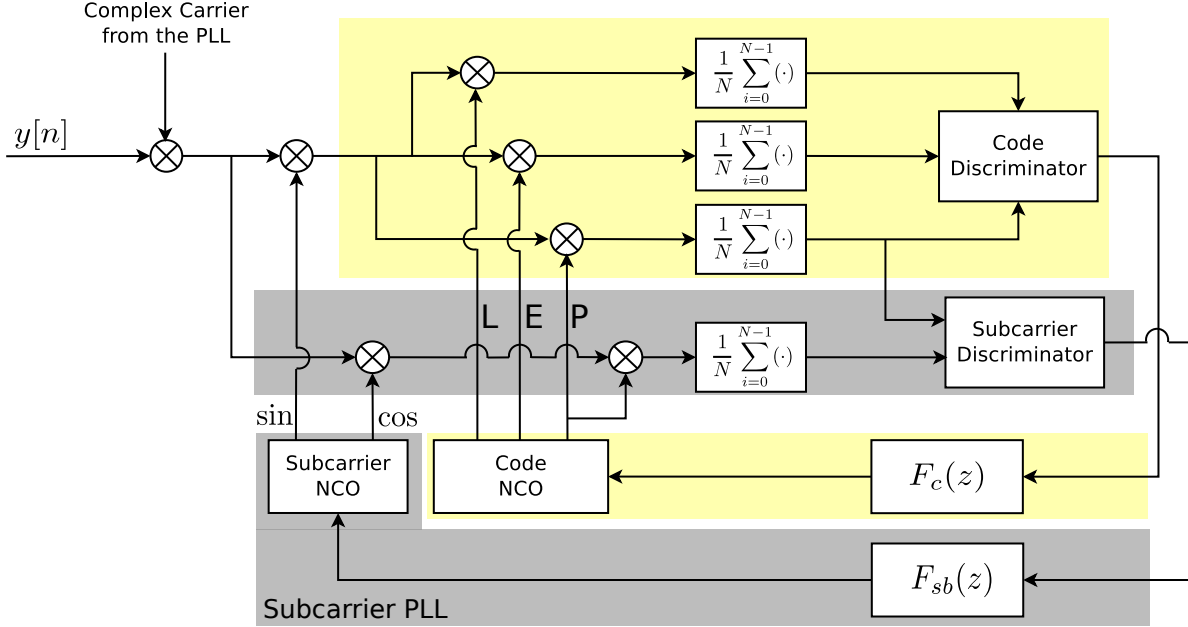
Fig. 1. Schematic representation of the DPE. A PLL is used to track the subcarrier component.

The residual carrier is at first removed from the input samples which are then multiplied by two orthogonal sinusoidal waves:

$$\bar{s}_b(nT_s) = \sqrt{2}\sin\left(2\pi\bar{f}_{sb}nT_s - \bar{\varphi}_{sb}\right)$$
$$\bar{s}_b^o(nT_s) = \sqrt{2}\cos\left(2\pi\bar{f}_{sb}nT_s - \bar{\varphi}_{sb}\right) \tag{7}$$

where $\bar{f}_{sb}$ is the estimated subcarrier frequency and accounts for the subcarrier nominal frequency, $f_{sb} = mf_r$, and the Doppler effect. The factor $\sqrt{2}$ is introduced in order to normalize the power of the waves in (7) to 1. The signal, $\bar{s}_b(nT_s)$, is an approximation of the received subcarrier and $\bar{\varphi}_{sb}$ is used to align the received and locally generated components. More specifically,

$$\bar{\varphi}_{sb} = 2\pi\bar{f}_{sb}\bar{\tau}, \tag{8}$$

where $\bar{\tau}$ is the estimated subcarrier delay. The wave, $\bar{s}_b^o(nT_s)$, is orthogonal to the local subcarrier and is required for the computation of an additional correlator which is used by the SPLL.

The signal obtained from the multiplication by $\bar{s}_b(nT_s)$ is used to compute the Early, Prompt and Late correlators which are required to evaluate the DLL discriminator output. In Fig. 1, N is the number of samples used for computing a complex correlator and $T_c = NT_s$ is the coherent

integration time. The Early, Prompt and Late correlators are given by

$$P = \frac{1}{N} \sum_{i=0}^{N-1} y[n] c\left(nT_s - \tau\right) \bar{s}_b(nT_s) \exp\{-j2\pi f_d nT_s - j\varphi\}$$

$$E = \frac{1}{N} \sum_{i=0}^{N-1} y[n] c\left(nT_s - \tau - d_s/2\right) \bar{s}_b(nT_s) \exp\{-j2\pi f_d nT_s - j\varphi\} \qquad (9)$$

$$L = \frac{1}{N} \sum_{i=0}^{N-1} y[n] c\left(nT_s - \tau + d_s/2\right) \bar{s}_b(nT_s) \exp\{-j2\pi f_d nT_s - j\varphi\}$$

where f_d and φ are carrier frequency and phase estimated by the carrier PLL. τ is the code delay estimated by the DLL at the previous iteration and d_s is the Early-minus-Late chip spacing. The correlators in (9) are used by the DLL as in standard GNSS receivers [22], [23] and for this reason DLL operations are not discussed further.

The signal obtained from the multiplication by $\bar{s}_b^o(nT_s)$ is used to compute an additional correlator

$$P_Q = \frac{1}{N} \sum_{i=0}^{N-1} y[n] c\left(nT_s - \tau\right) \bar{s}_b^o(nT_s) \exp\{-j2\pi f_d nT_s - j\varphi\}. \qquad (10)$$

Assuming perfect code and frequency synchronization, i.e, $\tau = \tau_0$ and $f_d = f_0$, it is possible to show that P and P_Q can be expressed as

$$P = \frac{\sqrt{C} s_1}{\sqrt{2}} d \exp\left\{j\Delta\varphi\right\} \frac{\sin\left(\pi\Delta f_{sb} N T_s\right)}{N \sin\left(\pi\Delta f_{sb} T_s\right)} \cos\left(\pi\Delta f_{sb}(N-1)T_s + \Delta\varphi_{sb}\right) + \eta_P$$

$$P_Q = \frac{\sqrt{C} s_1}{\sqrt{2}} d \exp\left\{j\Delta\varphi\right\} \frac{\sin\left(\pi\Delta f_{sb} N T_s\right)}{N \sin\left(\pi\Delta f_{sb} T_s\right)} \sin\left(\pi\Delta f_{sb}(N-1)T_s + \Delta\varphi_{sb}\right) + \eta_Q \qquad (11)$$

where d models the effect of the navigation message[1], s_1 is the first coefficient of the series expansion (5) and $\Delta\varphi = \varphi_0 - \varphi$ is the residual phase to be estimated by the PLL. The residual subcarrier frequency and phase are defined as

$$\Delta f_{sb} = f_{sb} - \bar{f}_{sb} \qquad (12)$$

$$\Delta\varphi_{sb} = 2\pi f_{sb}\tau_0 - \bar{\varphi}_{sb} = 2\pi\left(f_{sb}\tau_0 - \bar{f}_{sb}\bar{\tau}\right) \qquad (13)$$

and need to be recovered by the SPLL. η_P and η_Q are two complex circularly symmetric independent Gaussian random variables with zero mean and variance

$$\mathrm{Var}\left\{\eta_P\right\} = \mathrm{Var}\left\{\eta_Q\right\} = \frac{2}{N}\sigma^2. \qquad (14)$$

---

[1]it is assumed that $d(\cdot)$ takes a constant value over the integration period.

The independence of η_P and η_Q derives from the fact that they are the projections of $\eta_{BB}[n]$ over two orthogonal signals, $\bar{s}_b(nT_s)$ and $\bar{s}_b^o(nT_s)$.

For a small residual subcarrier frequency error,

$$\Delta f_{sb} \approx 0,$$

the complex correlators (11) can be further simplified as

$$P = \sqrt{\frac{C}{2}} s_1 d \exp\{j\Delta\varphi\} \cos(\Delta\varphi_s) + \eta_I$$
$$P_Q = \sqrt{\frac{C}{2}} s_1 d \exp\{j\Delta\varphi\} \sin(\Delta\varphi_s) + \eta_Q. \tag{15}$$

From (15), it is finally possible to design subcarrier discriminators able to generate the error signal used by the SPLL to maintain lock and estimate the subcarrier parameters. In particular, two classes of SPLL discriminators can be designed:

- **coherent discriminators**: the effect of the residual carrier phase is neglected ($\Delta\varphi = 0$) and the SPLL operates assuming perfect carrier synchronization. This is the same hypothesis adopted for coherent DLL discriminators [22].

- **non-coherent discriminators**: the subcarrier discriminator is designed to operate even in the presence of residual carrier phase errors ($\Delta\varphi \neq 0$).

The design of SPLL discriminators is out of the scope of this paper and only two discriminator examples are considered in the following. More specifically,

$$\epsilon_c(\Delta\varphi_s) = \arctan\left(\frac{\Re\{P_Q\}}{\Re\{P\}}\right) \tag{16}$$

can be used as coherent discriminator. When $\Delta\varphi = 0$, the signal components of P and P_Q are real and thus only the real parts of correlators (15) are used to compute the error signal, ϵ_c. Discriminator (16) is analogous to the Costas discriminator used in standard PLL. Other coherent discriminators can be obtained using different approximations for the arctangent function in (16). A non-coherent discriminator can be obtained as

$$\epsilon_{nc}(\Delta\varphi_s) = \arctan\left(\Re\left\{\frac{P_Q}{P}\right\}\right). \tag{17}$$

The working principle of (17) can be intuitively understood by neglecting the noise components, η_I and η_Q, in (15) and computing the ratio $\frac{P_Q}{P}$. Under this hypothesis, it clearly emerges that ϵ_{nc} is insensitive to residual carrier phase variations and equals $\Delta\varphi_s$. The noise performance of

(16) and (17) are analyzed in Section IV.

The discriminator output is then filtered and a new estimate of the subcarrier frequency, $\bar{f}_{sb}$, is produced. The transfer function of the SPLL loop filter is is denoted $F_{sb}(z)$ in Fig. 1. Note that the loop filter can be designed using standard techniques [22], [24]. As for standard PLLs, the subcarrier residual phase, $\Delta\varphi_{sb}$, is driven to zero by adjusting the estimated subcarrier frequency, $\bar{f}_{sb}$. The new estimate of $\bar{f}_{sb}$ is used by the Numerically Controlled Oscillator (NCO) of the SPLL to generate the local subcarriers, $\bar{s}_{sb}(\cdot)$ and $\bar{s}_{sb}^{o}(\cdot)$, closing the subcarrier processing loop of the DPE.

IV. PERFORMANCE ANALYSIS

In this section, the performance of the DPE are analyzed in terms of coherent output SNR and tracking jitter. The coherent output SNR [21], [25] is the ratio between the signal and noise power at the correlator output when the local signal replicas are perfectly aligned with the input signal. The tracking jitter [19] quantifies the amount of noise transferred by a tracking loop from the input signal to the final delay estimate. In this case, the tracking jitter of the SPLL is compared with that of the SLL of the DE, showing the advantages of the DPE. The tracking jitter of the SCC technique is also used as term of comparison.

A. Coherent Output SNR

The coherent output SNR is defined as [21], [25]:

$$SNR_q = \max_{\tau, f_d, \bar{\tau}} \frac{|\mathrm{E}\{P\}|^2}{\frac{1}{2}\mathrm{Var}\{P\}} \tag{18}$$

where the factor $\frac{1}{2}$ accounts for the fact that P is a complex quantity and only the power of its real part is considered. Using (15) and (14), it this possible to evaluate (18) when the sinusoidal subcarrier (7) is used to compute the prompt correlator:

$$SNR_q = \frac{C}{\frac{1}{N}N_0 B_{Rx}} \frac{s_1^2}{2}. \tag{19}$$

The term $\frac{s_1^2}{2}$ is the square modulus of the correlation between the input filtered subcarrier and $\bar{s}_b(nT_s)$, when the signal and estimated delays are aligned:

$$\left|\bar{R}(0)\right|^2 = \left|\frac{1}{N}\sum_{n=0}^{N-1} \tilde{s}_b\left(nT_s - \tau_0\right)\bar{s}_b(nT_s)\right|^2_{\bar{\tau}=\tau_0} = \frac{s_1^2}{2}. \tag{20}$$

The DE adopts a local subcarrier equal to the unfiltered ideal subcarrier $s_b \left(nT_s - \bar{\tau} \right)$. In this case, the coherent output SNR assumes the following form

$$SNR_{id} = \frac{C}{\frac{1}{N} N_0 B_{Rx}} \left| \tilde{R}(0) \right|^2 \tag{21}$$

where

$$\left| \tilde{R}(0) \right|^2 = \left| \frac{1}{N} \sum_{n=0}^{N-1} \tilde{s}_b \left(nT_s - \tau_0 \right) s_b \left(nT_s - \tau_0 \right) \right|^2. \tag{22}$$

The loss experienced when using a sinusoidal wave for recovering the signal subcarrier is thus given by the ratio between (20) and (22):

$$L_o = \frac{\left| \bar{R}(0) \right|^2}{\left| \tilde{R}(0) \right|^2}. \tag{23}$$

The worst case scenario occurs when $\tilde{s}_b(t) = s_b(t)$ and

$$L_o = \frac{s_1^2}{2}. \tag{24}$$

In the case of BOC subcarriers, $s_b(t)$, is a perfect square wave and $s_1 = \frac{4}{\pi}$. In this way, the worst loss which may be experienced is

$$L_o = \frac{8}{\pi^2} \quad \rightarrow \quad L_o|_{\text{dB}} = -0.91 \text{ dB} \tag{25}$$

that is less than 1 dB. Loss (25) is the same experienced by a GNSS receiver when processing the incoming carrier using a square wave approximation [26]. Note that L_o can become a gain when the signal is heavily filtered and $\tilde{s}_b(t)$ is more similar to a sinusoidal wave than to the ideal subcarrier. In this case, the correlation performed using a sinusoidal local subcarrier provides a better approximation of a filter matched to the input signal. This fact clearly emerges in Fig. 2 where the coherent output SNR loss is shown as a function of the front-end bandwidth. More specifically, a 9th order Butterworth filter was used to simulate the impact of front-end filtering and L_o was evaluated as a function of its cut-off frequency. The cases of sine BOC(1, 1) and cosine BOC(15, 2.5) are considered. From Fig. 2 it emerges that the DPE provides a gain for the processing of wide-band BOC modulated signals. This is the case of the cosine BOC(15, 2.5) modulation adopted for the Galileo PRS: a front-end with a total bandwidth greater than 45 MHz is required to obtain an actual loss. Note that signal band-limiting can also be introduced at the transmitter side. For example, the cosine BOC(15, 2.5) transmitted by the GIOVE-B satellite was characterized by a bandwidth of about 40 MHz [27]. In this case, the DPE will always provided better performance with respect to standard techniques.
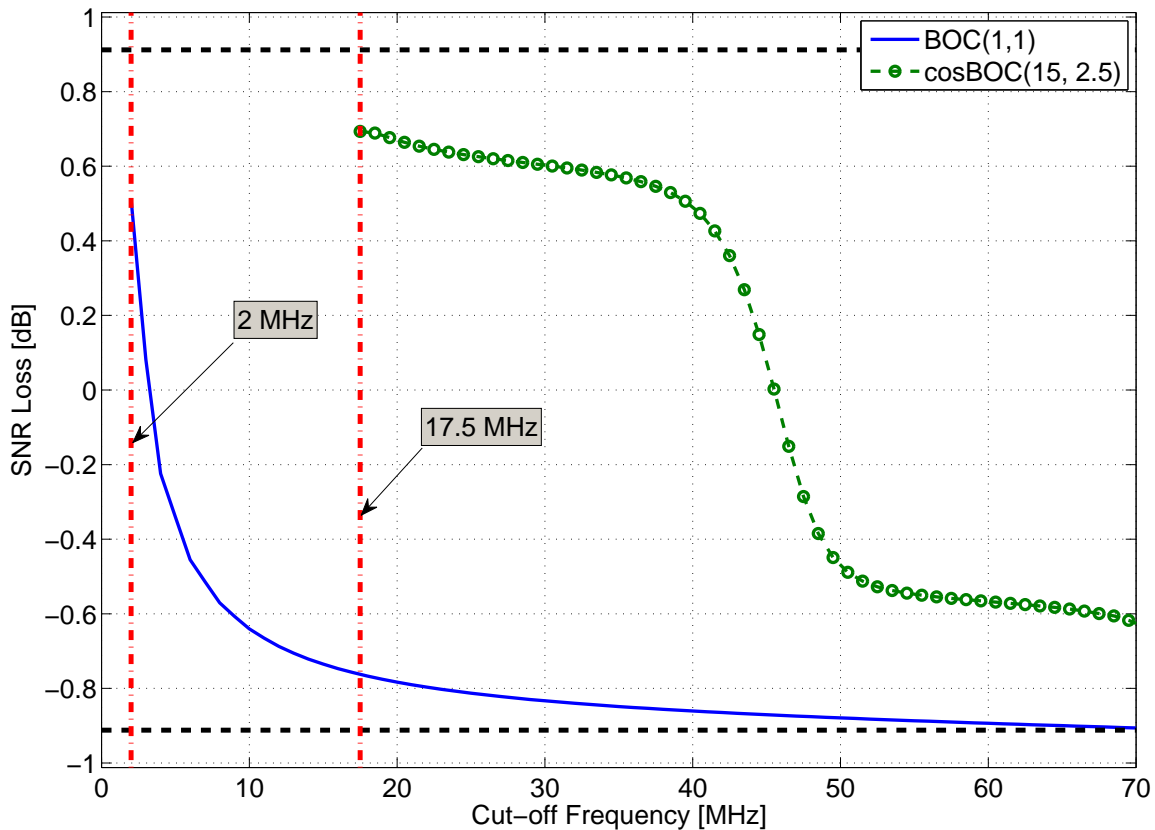
Fig. 2. Coherent output SNR loss for the sine BOC(1, 1) and cosine BOC(15, 2.5) as a function of the cut-off frequency of a Butterworth filter of order 9. The filter was used to simulate the effect of front-end filtering.

B. Tracking Jitter

In this section, the tracking jitter of the SPLL is derived and compared with that of the SLL employed by the DE. The SCC technique is also used as term of comparison. In the DE, the final delay estimate is obtained as a function of the subcarrier and code delays. When considering the DE approach, it is possible to show [16], [18] that the dominant contribution to the jitter of the final delay estimate is from the SLL. The final tracking jitter can thus be effectively approximated by that of the subcarrier delay estimate [16], [18]. The SCC tracking jitter can be compared with that of the SLL and SPLL under this approximation which allows comparison among different loops.

The tracking jitter can be computed as [23]

$$\sigma_\tau = \frac{\sigma_d}{G_d}\sqrt{2B_{eq}T_c} \tag{26}$$

where σ_d is the standard deviation of the discriminator output, B_{eq} is the loop equivalent bandwidth and T_c is the coherent integration time introduced in Section III. G_d is the discriminator gain defined as

$$G_d = \left.\frac{\partial \mathrm{E}\left[S(\tau)\right]}{\partial \tau}\right|_{\tau=0} \tag{27}$$

where $S(\cdot)$ is the discriminator input-output function. $S(\cdot)$ depends on the type of discriminator and can be computed using definitions (16) and (17) and correlator model (15). In both coherent and non-coherent case, it is possible to show

$$S(\tau) = 2\pi f_{sb}\tau + \eta_\tau \tag{28}$$

where η_τ is a zero mean residual noise term the statistics of which depend on the type of discriminator. For the coherent discriminator, (16), the tracking jitter can be computed using an approach similar to that developed in [28] for the evaluation of the normalized standard deviation at the output of an arctangent discriminator. In particular, it is possible to show that

$$\frac{\sigma_d}{G_d} = \frac{1}{2\pi f_{sb}}\sqrt{\frac{SNR_q+1}{SNR_q^2}} = \frac{1}{2\pi f_{sb}}\sqrt{\frac{1}{\frac{C}{\frac{1}{N}N_0B_{Rx}}L_o}\left(1 + \frac{1}{\frac{C}{\frac{1}{N}N_0B_{Rx}}L_o}\right)}. \tag{29}$$

The normalization factor, $\frac{1}{2\pi f_{sb}}$, is used to express the normalized standard deviation in units of seconds accounting for the fact that the output of (16) is in units of cycles. From (29), it is finally possible to compute the tracking jitter of the coherent discriminator:

$$\sigma_\tau = \frac{1}{2\pi f_{sb}}\sqrt{\frac{2B_{eq}T_c}{\frac{C}{\frac{1}{N}N_0B_{Rx}}\frac{s_1^2}{2}}\left(1 + \frac{1}{\frac{C}{\frac{1}{N}N_0B_{Rx}}\frac{s_1^2}{2}}\right)} \approx \frac{1}{2\pi f_{sb}}\sqrt{\frac{B_{eq}}{\frac{C}{N_0}\frac{s_1^2}{2}}\left(1 + \frac{1}{2\frac{C}{N_0}T_c\frac{s_1^2}{2}}\right)} \tag{30}$$

where the last approximation was obtained exploiting the hypothesis

$$B_{Rx} \approx \frac{f_s}{2} = \frac{1}{2T_s} \rightarrow \frac{1}{N}B_{Rx} \approx \frac{1}{2NT_s} = \frac{1}{2T_c}. \tag{31}$$

The tracking jitter for the non-coherent discriminator can be computed using the approach described in Appendix I where it is shown that for high coherent output SNR values, the non-coherent discriminator is equivalent to the coherent one after that the residual carrier phase error has been compensated for. Given the equivalence of these two discriminators for a high coherent

TABLE I

Parameter	Value
Sampling Frequency, f_s	8 MHz
Integration Time, T_c	4 ms
Modulation Type	sine BOC(1, 1)
DLL Order	1st
DLL Bandwidth	1 Hz
SPLL Order	1st

output SNR, it is possible to conclude that the two discriminators lead to the same tracking jitter. Note that the equivalence is valid only for high SNR conditions and better performance is expected for the coherent discriminator for low SNR values.

The validity of (30) is investigated in the following using a semi-analytic approach [16], [29]. More specifically, the same approach adopted in [29] to evaluate the tracking jitter of the DE was adopted to characterize the performance of the DPE. In a semi-analytic framework, the knowledge of the system is used to alleviate the computation requirements that full Monte Carlo simulations would require. In this case, theoretical models are used for the generation of the correlator outputs whereas the non-linear components of the system are fully simulated [30]. The simulation parameters adopted for the analysis of the DPE are provided in Table I. In particular, a system consisting of a first order DLL and a first order SPLL was considered. The integration time was set to 4 ms that is the duration of a code period of the Galileo E1c/E1b signal. The DLL bandwidth was set to 1 Hz whereas different SPLL bandwidths were considered.

Results relative to the coherent discriminator are shown in Fig. 3 where (30) is compared with simulation results. In Fig. 3, the tracking jitter is provided as function of the input C/N_0 and for different loop bandwidths and is expressed in units of meters. Jitter (30) is in units of seconds and the conversion in meters is obtained through the multiplication by the speed of light. In all cases considered, a good match between theoretical and simulation results is found supporting the validity of (30). It is noted that the curve relative to $B_{eq} = 5$ Hz experiences a sudden jump for a C/N_0 equal to 24 dB-Hz. This effect is due to the fact that the SPLL is loosing lock and is thus unable to provide valid subcarrier delay estimates. Formula (30) was obtained exploiting
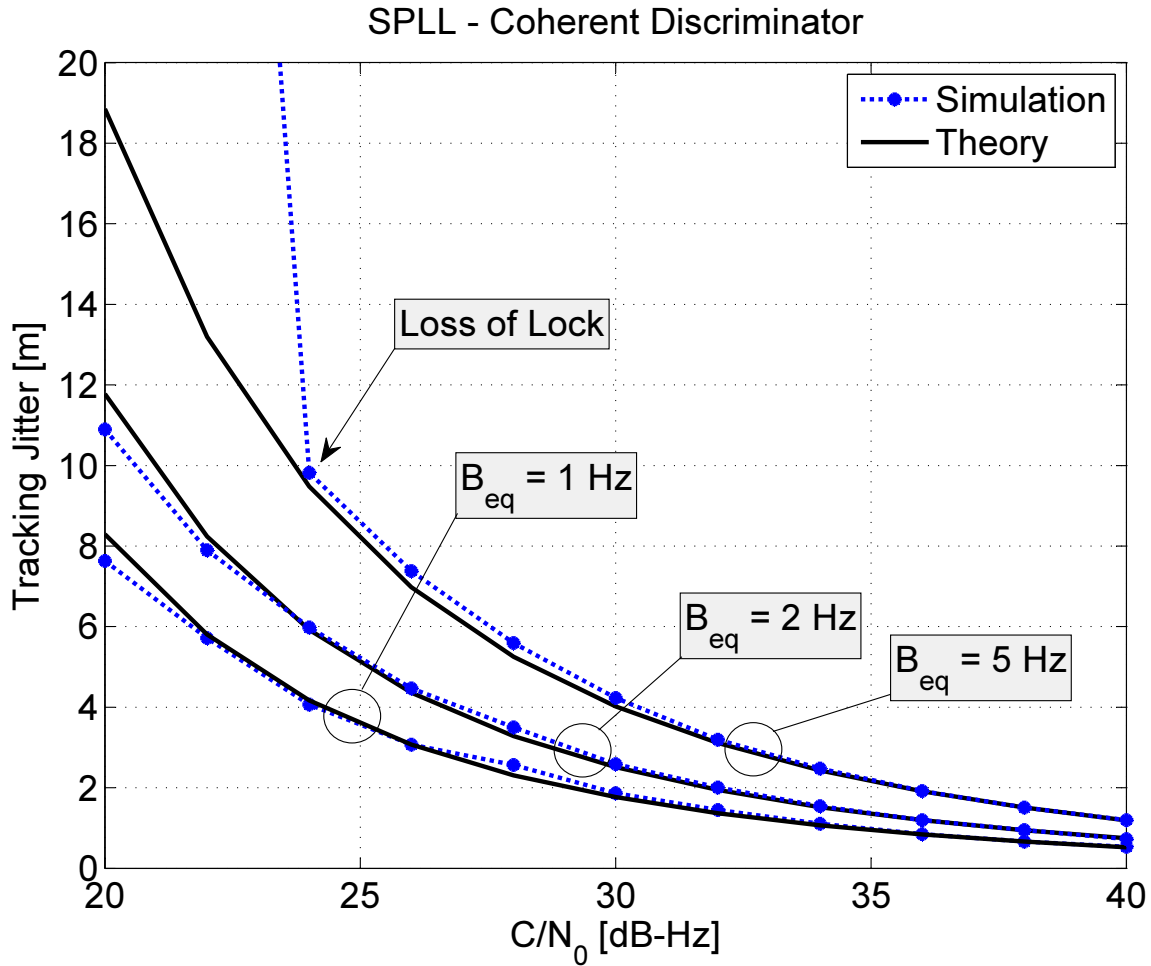
Fig. 3. Tracking jitter of the SPLL with coherent discriminator for different loop bandwidths. Comparison between simulations and theoretical results.

a linear approximation of the loop and thus is unable to predict non-linear phenomena such as loss of lock. Lower equivalent bandwidths better shield the loop against the input noise and loss of lock does not occur. Deviations of the simulation curves from theoretical results at low C/N_0 values are also due to non-linear effects which are not accounted by (30) [29].

The non-coherent discriminator is considered in Fig. 4 where the tracking jitter is depicted as a function of the input C/N_0 and for different equivalent loop bandwidths, B_{eq}. Also in this case, a good agreement between theoretical and simulation results is observed. The performance of the non-coherent discriminator is very close to that of the coherent discriminator as predicted by the derivations provided in Appendix I.
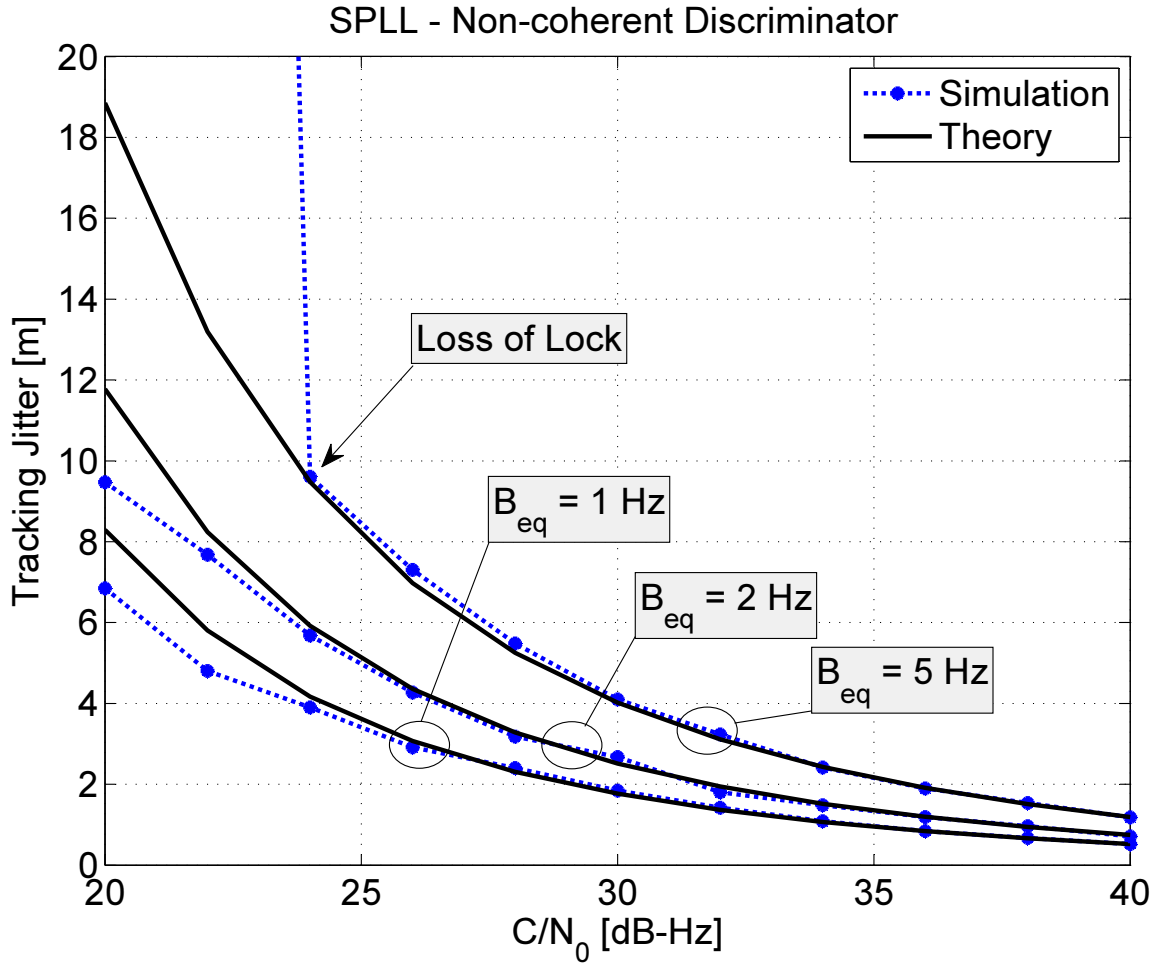
Fig. 4. Tracking jitter of the SPLL with non-coherent discriminator for different loop bandwidths. Comparison between simulations and theoretical results.

The results provided in Figs. 3 and 4 support the effectiveness of (30) which is able to predict the tracking jitter of the SPLL as a function of the different system and signal parameters. Although only the case of a sine BOC(1, 1) is analyzed in the paper, similar results were obtained for higher order modulations.

The tracking jitters of the DE SLL and of the SCC are considered in the following as terms of comparison for the performance of the SPLL. The tracking jitter of an SLL using a non-coherent
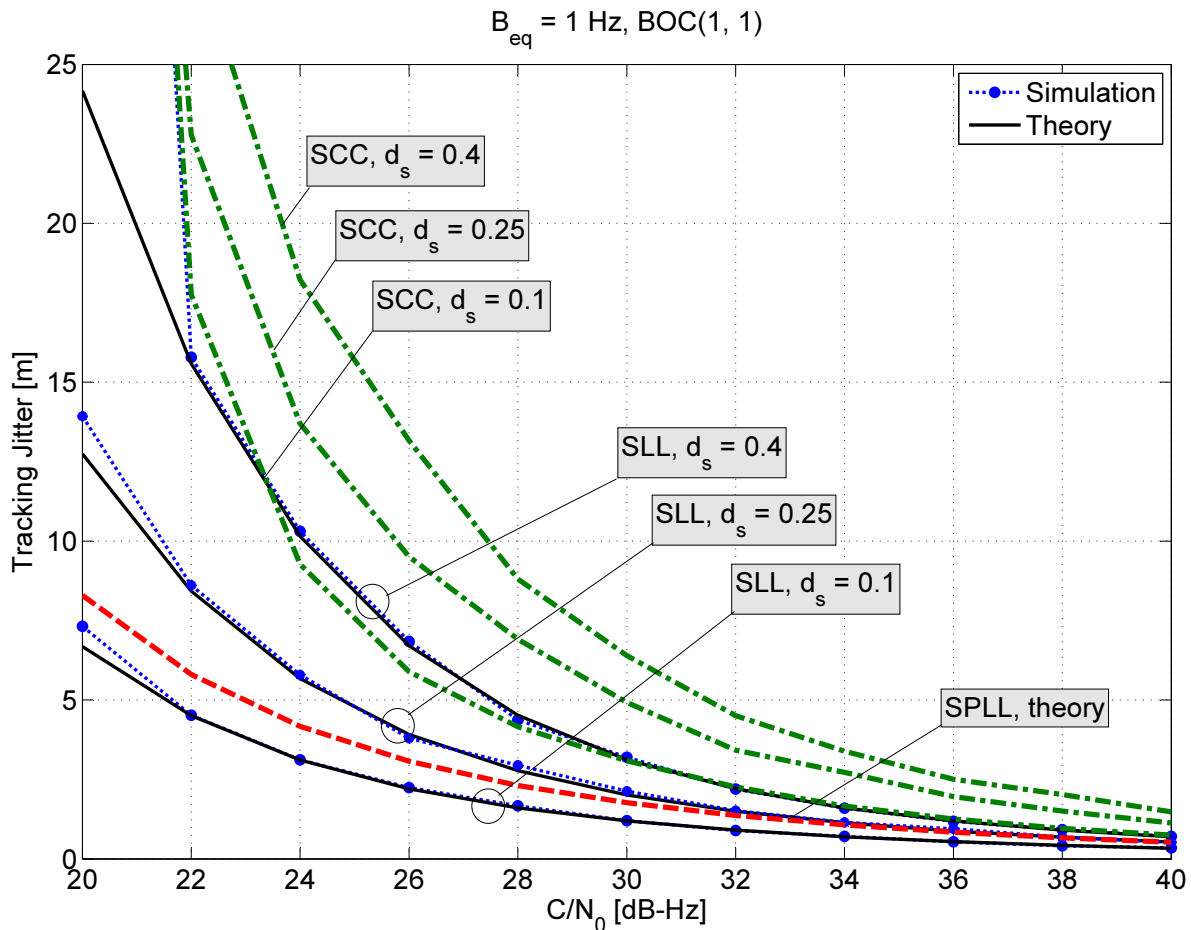
Fig. 5. Comparison between the SLL and the SPLL in terms of tracking jitter. Different SLL Early-minus-Late chip spacings are considered. Simulation results for the SCC techniques are also provided as additional term of comparison.

discriminator was derived in [14] (Appendix A) and assumes the following form

$$\sigma_\tau^{SLL} = \frac{1}{f_{sb}} \sqrt{\frac{B_{eq} d_s}{8 C/N_0} \left(1 + \frac{1}{\frac{C}{N_0} T_c (1 - 2 d_s)}\right)} \qquad (32)$$

where d_s is the SLL Early-minus-Late spacing expressed in subcarrier periods, $T_{sb} = \frac{1}{f_{sb}}$. Note that, due to the periodicity of the subcarrier, the following condition applies

$$d_s < 0.5$$

i.e., the subcarrier Early and Late correlators have to be computed using local subcarriers with a relative delay lower than $0.5 T_{sb}$. The tracking jitter of the SLL is compared with that of the SPLL in Fig. 5. The performance of the SLL strongly depends on the Early-minus-Late spacing

adopted: for narrow d_s, the SLL outperforms the SPLL which becomes preferable for d_s greater than 0.25. For $d_s = 0.25$, the SLL and SPLL have similar performance as predicted by (30) and (32) when $L_o = \frac{s_1^2}{2} = \frac{8}{\pi^2}$. It is noted that a narrow d_s reduces the ability of the SLL to recover large initial delay errors and strongly impacts the transient behavior of the loop. The transient analysis of SLL and SPLL is beyond the scope of this paper.

Fig. 5 also provides the tracking jitter of the DLL of the SCC technique. Since no theoretical results are currently available on the SCC tracking jitter [12], [13], [15], only simulation results are presented. The algorithm detailed in [13] was implemented and used for the analysis: SCC also requires the computation of Early and Late subcarrier correlators and the performance of the loop strongly depends on the Early-minus-Late chip spacing, d_s. From the results provided in Fig. 5, it emerges that the SPLL achieves performance similar to that of the SLL even if it requires a lower computational load. Note that the analysis presented above assumed ideal front-end filtering. Under this condition, the SLL achieves its best performance whereas the SPLL experiences the worst loss. Even in this case, the SPLL achieves satisfactory performance in terms of tracking jitter. Improved performance is expected in the presence of front-end filtering. The SCC is always outperformed by the other techniques as already remarked by [15]. This fact is expected and is due to the subcarrier removal operated by the SCC technique. Although the SCC uses a sinusoidal representation of the subcarrier, its performance is significantly worse than that of the DPE.

V. REAL DATA ANALYSIS

In the previous section, the performance of the DPE was analyzed in terms of coherent output SNR and tracking jitter. Semi-analytic simulations were also used to support the validity of theoretical results. In this section, real data collected using a wide-band Radio Frequency Signal Analyzer (RFSA) are used to demonstrate the feasibility of the proposed tracking technique and further investigate the performance of the DPE. More specifically, a National Instruments (NI) PXI-e 5663 vector signal analyzer was used to collect data from the GIOVE-B satellite. It is noted that the GIOVE-B satellite was decommissioned in the Summer 2012 and that the data set used in this paper was collected on 5th November 2011. The use of such data set is justified by the fact that it contains valid cosine BOC(15, 2.5) data with a known Pseudo Random Noise (PRN) code [31]. Thus, the use of this data set allows one to test the DPE for both the sine

TABLE II

PARAMETERS ADOPTED FOR THE COLLECTION OF WIDE-BAND GIOVE-B SIGNALS.

Parameter	Value
Sampling Frequency	$f_s = 40$ MHz
Sampling Type	Complex I&Q
Centre Frequency	1575.42 MHz
No. of bits	16

BOC(1, 1) and cosine BOC(15, 2.5) modulation broadcast in the Galileo E1 band. The cosine BOC(15, 2.5) transmitted by the currently operating Galileo satellites is encrypted and requires the use of codeless techniques [32]. The use of GIOVE-B signals allows one to demonstrate the effectiveness of the DPE using real data providing an analysis complementary to that based on simulations and discussed in Section IV.

The parameters adopted for the data collection are reported in Table II. The NI signal analyzer has a bandwidth of about 38 MHz and is able to capture the main lobes of the cosine BOC(15, 2.5) modulation. The parameters adopted for the processing of the E1a and E1c signals are reported in Table III. Both DE and DPE were implemented and the same parameters (loop bandwidth, order and integration time) were used to allow a fair comparison. The E1a signal is characterized by a primary code duration of 2 ms and a secondary code of 5 elements. After the recovery of the secondary code, the integration time is increased from 2 to 10 ms. For the E1c signal, the integration time is kept constant to 8 ms, the duration of one code period.

Sample results relative to the processing of GIOVE-B signals are provided in the following. The DPE is able to effectively process the E1a signal and sample results are provided in Fig. 6 which shows several metrics indicating the proper functioning of the technique proposed. The amplitudes of the Prompt, Early and Late correlators used by the DLL coupled with the SPLL are shown in Fig. 6a): after an initial transient period, the amplitude of the Prompt correlator is maximized whereas Early and Late assume similar magnitudes. In Fig. 6b) the filter outputs of the 3 loops used for signal tracking are provided. Each output is normalized by the fundamental frequency of the component tracked: the carrier Doppler is normalized by the GPS L1 centre frequency, 1575.42 MHz, the DLL filter output by the nominal code rate, 2.5575 MHz, and the

TABLE III

Parameter	Value
PLL order	3
PLL bandwidth	10 Hz
DLL order	2
DLL bandwidth	5 Hz
DLL Early-minus-Late chip spacing	0.5 chips
SPLL order	2
SPLL bandwidth	5 Hz
SLL order	2
SLL bandwidth	5 Hz
SLL Early-minus-Late spacing	$0.25T_{sub}$
E1a Integration Time (before bit synch)	2 ms
E1a Integration Time (after bit synch)	10 ms
E1c Integration Time	8 ms

SPLL filter output by the subcarrier rate, 15.345 MHz. The normalized filter outputs assume similar values indicating the possibility of carrier aiding: the normalized carrier Doppler can be used to aid the processing of the code and subcarrier components. As expected the code estimates are the nosiest. After about 2 seconds, the secondary code on the E1a signal is recovered and bit synchronization is achieved. Thus, the integration time is increased from 2 to 10 ms. This fact can be clearly seen in the code rate estimates in Fig. 6b) and in Fig. 6c) which shows the in-phase and quadrature components of the E1a Prompt correlators. After bit synchronization, the secondary code is removed and the navigation bits can be extracted from the in-phase components of the Prompt correlators. Finally, the magnitude of the P_Q correlator is compared with that of the Prompt correlator in Fig. 6d). After an initial transient, the magnitude of P_Q is minimized and all the signal energy is concentrated in the Prompt correlator. This shows the ability of the DPE to properly track the different components of the cosine BOC(15, 2.5) modulation.

The correlators extracted by the DPE were used to estimate the C/N_0 of the GIOVE-B E1a signal using the Wide Band vs. Narrow Band (WBNB) approach [23]. C/N_0 estimates were also obtained using the correlators provided by the DE and sample results are shown in Fig. 7 along
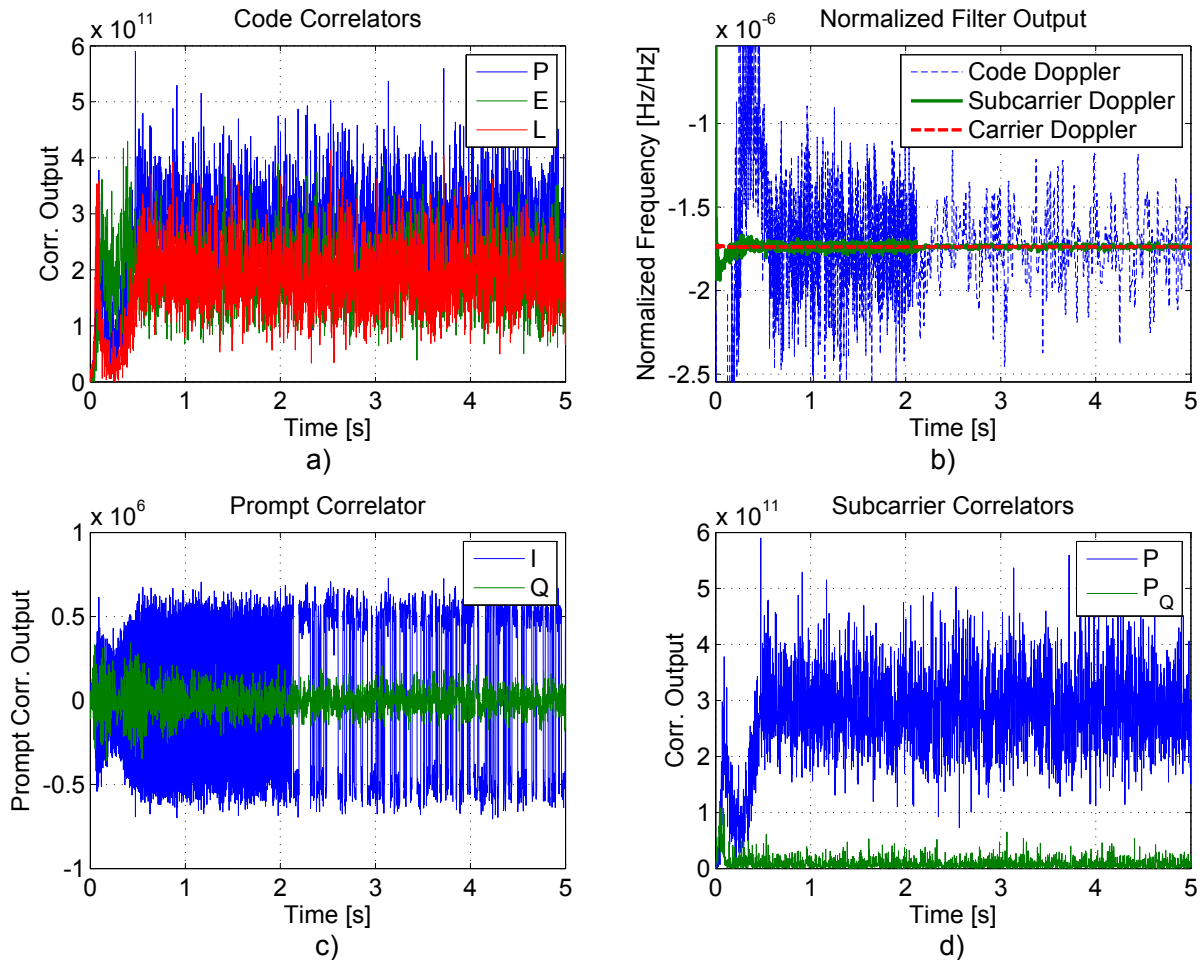
Fig. 6. Processing of the GIOVE-B cosine BOC(15, 2.5) using the DPE. a) Amplitude of the Prompt, Early and Late correlators used by the DLL. b) Normalized filter outputs of the three loops used for signal tracking. c) In-phase and quadrature components of the prompt correlator output. d) Amplitude of the P and P_Q correlators.

with the C/N_0 estimates relative to the DPE. The superiority of the DPE in the presence of signal bandlimiting clearly emerges from Fig. 7 which shows that a 0.87 dB C/N_0 improvement is achieved with respect to the DE. It is noted that the WBNB technique estimates an effective C/N_0 [25] that is a scaled version of the coherent output SNR analyzed in Section IV-A. In this respect, the results presented in Fig. 7 are in agreement with the theory detailed in Section IV-A which predicted the superiority of the DPE in the presence of front-end filtering.

Sample results relative to the processing of the sine BOC(1, 1) signals are shown in Fig. 8 which compares the C/N_0 estimates obtained using the DPE and DE for the same data set. In this case, the DPE experiences a 0.61 dB loss with respect to the DE as predicted by the theory
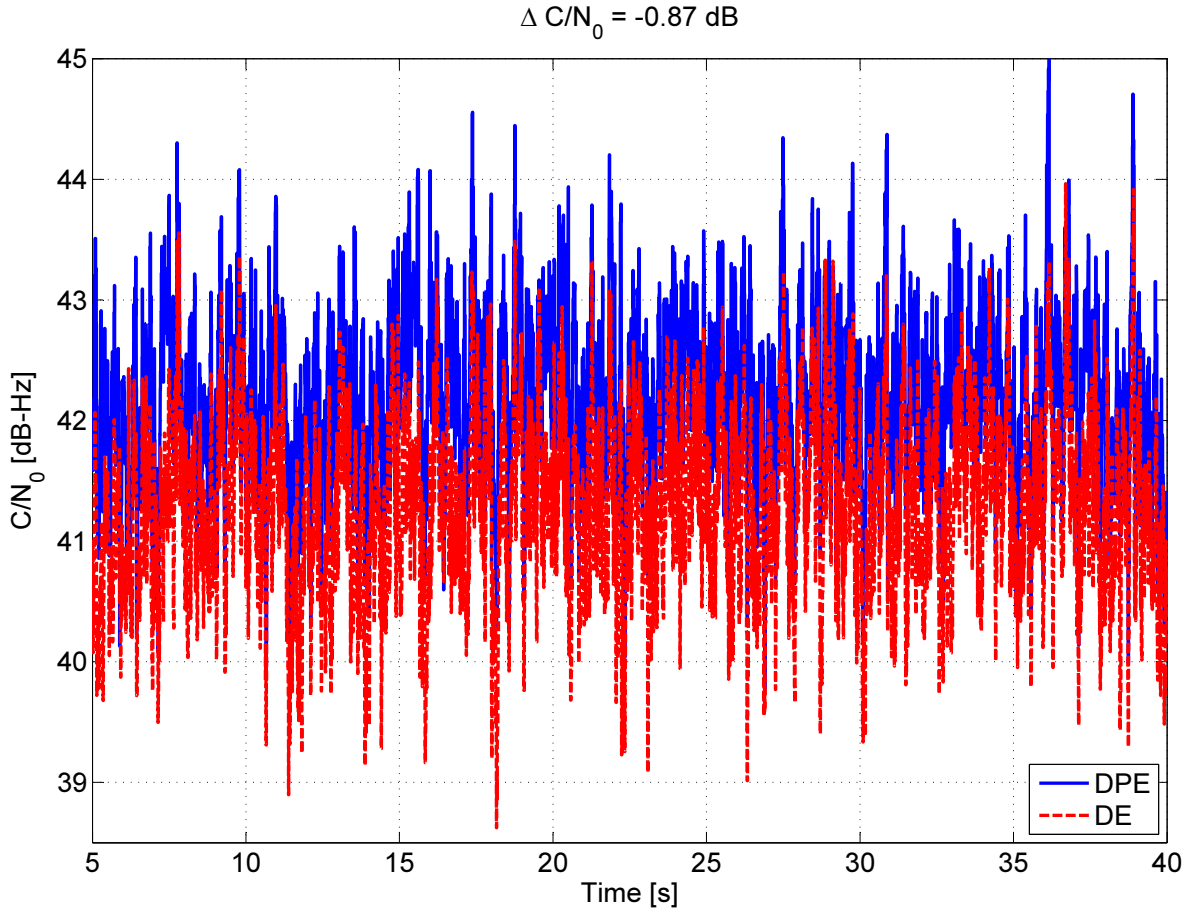
Fig. 7. C/N_0 estimates obtained using the DPE and DE for the GIOVE-B cosine BOC(15, 2.5) E1a signal. The DPE outperforms the DE and achieves a C/N_0 improvement of about 0.87 dB.

developed in Section IV-A. This loss is however quite small and is justified by the reduced computational load required by the DPE with respect to the DE.

These results illustrate the ability of the DPE to process different BOC signals and support the theoretical findings derived in Section IV.

VI. CONCLUSIONS

In this paper, a novel unambiguous BOC tracking algorithm has been proposed. The algorithm provides an alternative to the DE and replaces the SLL used for tracking the subcarrier component by a modified PLL, named SPLL. The use of the SPLL is justified by the fact that after front-end filtering, the subcarrier component can be effectively approximated by a pure sine wave.
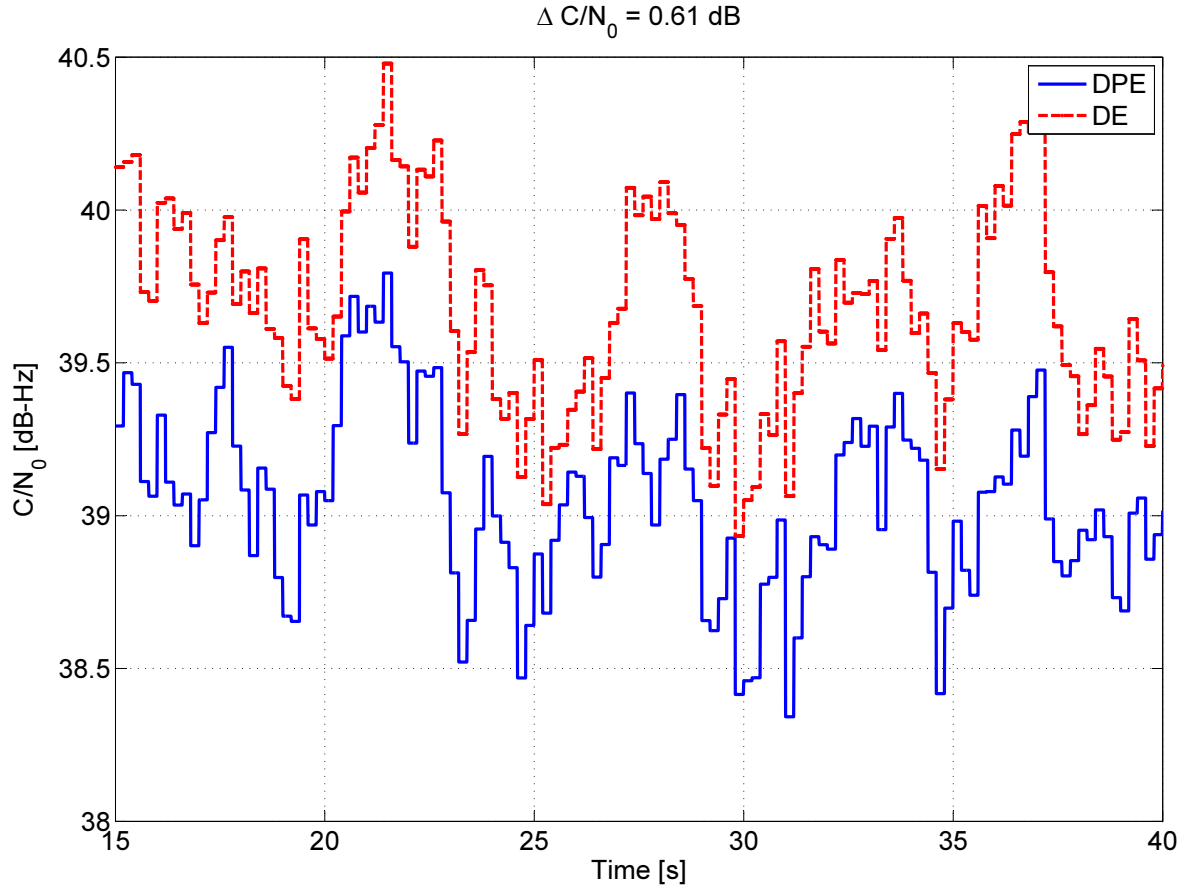
Fig. 8. C/N_0 estimates obtained using the DPE and DE for the GIOVE-B BOC(1, 1) E1c signal. The DPE experiences a 0.61 dB loss with respect to the DE.

The algorithm proposed, the DPE, if thoroughly characterized and its performance is determined under different operating conditions. In particular, it shown that the DPE outperforms the DE in the presence of front-end filtering. Theoretical results are supported by simulations and the effectiveness of the technique proposed is demonstrated by processing real wide-band BOC signals. The good agreement between theoretical, simulation and experimental results supports the validity of the findings presented. Finally, the DPE requires a lower computational load than the DE and thus should be preferred for example for the processing of wide-band signals such as the cosine BOC(15, 2.5) modulation.

APPENDIX I

NON-COHERENT DISCRIMINATOR

In this appendix, the properties of the non-coherent discriminator, (17), are briefly investigated. In particular, it is shown that for high coherent output SNR values, (17) is equivalent to the coherent discriminator, (16), after that the residual carrier phase, $\Delta\varphi$, has been compensated for. The non-coherent discriminator, (17), is defined as the arctangent of

$$\Re\left\{\frac{P_Q}{P}\right\} \tag{33}$$

which can be expressed as

$$
\begin{aligned}
\Re\left\{\frac{P_Q}{P}\right\} &= \Re\left\{\frac{P_Q \exp\{-j\Delta\varphi\}}{P \exp\{-j\Delta\varphi\}}\right\} \\
&= \Re\left\{\frac{\Re\{P_Q \exp\{-j\Delta\varphi\}\}}{\Re\{P \exp\{-j\Delta\varphi\}\}}\frac{1+j\rho_Q}{1+j\rho}\right\} \\
&= \frac{\Re\{P_Q \exp\{-j\Delta\varphi\}\}}{\Re\{P \exp\{-j\Delta\varphi\}\}}\Re\left\{\frac{1+j\rho_Q}{1+j\rho}\right\} \\
&= \frac{\Re\{P_Q \exp\{-j\Delta\varphi\}\}}{\Re\{P \exp\{-j\Delta\varphi\}\}}\Re\{(1+j\rho_Q)(1-j\rho)\}\frac{1}{1+\rho^2} \\
&= \frac{\Re\{P_Q \exp\{-j\Delta\varphi\}\}}{\Re\{P \exp\{-j\Delta\varphi\}\}}(1+\rho_Q\rho)\frac{1}{1+\rho^2}.
\end{aligned}
\tag{34}
$$

where

$$\rho_Q = \frac{\Im\{P_Q \exp\{-j\Delta\varphi\}\}}{\Re\{P_Q \exp\{-j\Delta\varphi\}\}} \qquad \rho = \frac{\Im\{P \exp\{-j\Delta\varphi\}\}}{\Re\{P \exp\{-j\Delta\varphi\}\}}. \tag{35}$$

Note that for high coherent output SNR values, i.e., when the signal component in (15) is dominant,

$$\rho \ll 1$$

and the last fraction in (34) can be expanded as a geometric series. In this way, (33) can be expressed as

$$
\begin{aligned}
\Re\left\{\frac{P_Q}{P}\right\} &= \frac{\Re\{P_Q \exp\{-j\Delta\varphi\}\}}{\Re\{P \exp\{-j\Delta\varphi\}\}}(1+\rho_Q\rho)\sum_{i=0}^{+\infty}\left(-\rho^2\right)^i \\
&= \frac{\Re\{P_Q \exp\{-j\Delta\varphi\}\}}{\Re\{P \exp\{-j\Delta\varphi\}\}}\left[1+\sum_{i=1}^{+\infty}\left(-\rho^2\right)^i + \rho_Q\rho\sum_{i=0}^{+\infty}\left(-\rho^2\right)^i\right].
\end{aligned}
\tag{36}
$$

If only the constant term in (36) is retained, the following approximation is finally obtained:

$$\Re\left\{\frac{P_Q}{P}\right\} \approx \frac{\Re\{P_Q \exp\{-j\Delta\varphi\}\}}{\Re\{P \exp\{-j\Delta\varphi\}\}}. \tag{37}$$

The truncation in (37) is justified by the hypothesis of a high coherent output SNR. Approximation (37) shows that, for high SNR values, the non-coherent discriminator is equivalent to the coherent discriminator after that the residual carrier phase error has been compensated for. For this reason, the coherent and non-coherent discriminators have the same tracking jitter for high SNR values.

REFERENCES

[1] Titus, B., Betz, J., Hegarty, C., Owen, R.: 'Intersystem and intrasystem interference analysis methodology'. Proc. of the 16th International Technical Meeting of the Satellite Division of The Institute of Navigation (ION GPS/GNSS), Portland, OR , September 2003, pp. 2061 – 2069

[2] ITU: 'Recommendation ITU-R M.1831, a coordination methodology for RNSS inter-system interference estimation', 2007

[3] Betz, J.W.: 'Binary offset carrier modulations for radionavigation'. NAVIGATION, the Journal of the Institute of Navigation, Winter 2001, 48, (4), pp. 227–246

[4] Rebeyrol, E., Julien, O., Macabiau, C., Ries, L., Delatour, A., Lestarquit, L.: 'Galileo civil signal modulations'. GPS Solutions, 2007, 11, pp. 159–171. ISSN 1080-5370

[5] Fine, P., Wilson, W.: 'Tracking algorithm for GPS offset carrier signal'. Proc. of the National Technical Meeting of The Institute of Navigation, San Diego, CA, January 1999, pp. 671–676

[6] Julien, O., Macabiau, C., Cannon, M., Lachapelle, G.: 'ASPeCT: unambiguous sine-boc(n,n) acquisition/tracking technique for navigation applications'. IEEE Trans. Aerosp. Electron. Syst., January 2007, 43, (1), pp. 150–162

[7] Burian, A., Lohan, E., Renfors, M.K.: 'Efficient delay tracking methods with sidelobes cancellation for BOC-modulated signals'. EURASIP Journal on Wireless Communications Networking, 2007, page 20. Article ID 72626

[8] Hodgart, M., Blunt, P.: 'Dual estimate receiver of binary offset carrier modulated signals for global navigation satellite systems'. Electronics Letters, 2 2007, 43, (16), pp. 877 –878. ISSN 0013-5194. doi:10.1049/el:20071101

[9] Hodgart, M.S., Blunt, P., Unwin, M.: 'The optimal dual estimate solution for robust tracking of binary offset carrier (BOC) modulation'. Proc. of the 20th International Technical Meeting of the Satellite Division of The Institute of Navigation (ION GNSS), Fort Worth, TX, September 2007, pp. 1017–1027

[10] Anantharamu, P., Borio, D., Lachapelle, G.: 'Sub-carrier shaping for BOC modulated GNSS signals'. EURASIP Journal on Advances in Signal Processing, 2011, 133, (1), pp. 1–18. ISSN 1687-6180. doi:10.1186/1687-6180-2011-133

[11] Lohan, E., Burian, A., Renfors, M.: 'Low-complexity unambiguous acquisition methods for BOC-modulated CDMA signals'. International Journal of Satellite Communications and Networking, October 2008, 26, (6), pp. 503–522

[12] Ward, P.W.: 'A design technique to remove the correlation ambiguity in binary offset carrier (BOC) spread spectrum signals'. Proc. of the National Technical Meeting of The Institute of Navigation, San Diego, CA, January 2004, pp. 886–896

[13] Ward, P.W., Lillo, W.E.: 'Ambiguity removal method for any GNSS binary offset carrier (BOC) modulation'. Proc. of the International Technical Meeting of The Institute of Navigation, Anaheim, CA, January 2009, pp. 406–419

[14] Anantharamu, P.: Space-Time Equalization Techniques for New GNSS Signals. Phd thesis, Schulisch School of Engineering, University of Calgary, September 2011

[15] Wendel, J., Hager, S.: 'A robust technique for unambiguous BOC tracking'. Proc. of the 26th International Technical Meeting of the Satellite Division of The Institute of Navigation (ION GNSS+), Nashville, TN, September 2013, pp. 1–12

[16] Anantharamu, P., Borio, D., Lachapelle, G.: 'Pre-filtering, side-peak rejection and mapping: Several solutions for unambiguous BOC tracking'. Proc. of the 22nd International Technical Meeting of The Satellite Division of the Institute of Navigation (ION GNSS), Savannah, GA, September 2009, pp. 3142–3155

[17] Palestini, C.: Synchronization and Detection Techniques for Navigation and Communication Systems. Phd thesis, University of Bologna, March 2010

[18] Ren, J., Jia, W., Chen, H., Yao, M.: 'Unambiguous tracking method for alternative binary offset carrier modulated signals based on dual estimate loop'. IEEE Commun. Lett., November 2012, 16, (11), pp. 1737–1740

[19] Van Dierendonck, A.J., Fenton, P., Ford, T.: 'Theory and performance of narrow correlator spacing in a GPS receiver'. NAVIGATION: Journal of the Institute of Navigation, Fall 1992, 39, (3), pp. 265 –283

[20] Betz, J.W., Kolodziejski, K.R.: 'Generalized theory of code tracking with an early-late discriminator part I: Lower bound and coherent processing'. IEEE Trans. Aerosp. Electron. Syst., October 2009, 45, (4), pp. 1538–1556. ISSN 0018-9251. doi:10.1109/TAES.2009.5310316

[21] Borio, D.: 'A statistical theory for gnss signal acquisition'. PhD Thesis, Politecnico di Torino, 2008

[22] Kaplan, E.D., Hegarty, C., editors. Understanding GPS: Principles and Applications. Artech House Publishers, Norwood, MA, USA 2005, 2nd edition

[23] Van Dierendonck, A.: 'Ch. 5, GPS receivers'. In B.W. Parkinson, J.J. Spilker Jr., editors, Global Positioning System Theory and Applications, volume 1. American Institute of Aeronautics & Astronautics 1996, pp. 329–407

[24] Stephens, S.A., Thomas, J.B.: 'Controlled-root formulation for digital phase-locked loops'. IEEE Trans. Aerosp. Electron. Syst., January 1995, 31, (1), pp. 78–95

[25] Betz, J.W.: 'Effect of partial-band interference on receiver estimation of C/N_0: Theory'. Proc. of the National Technical Meeting of The Institute of Navigation, Long Beach, CA, January 2001, pp. 817–828

[26] Borio, D.: 'Square wave decomposition for fast correlation in DSSS receivers'. IEEE Trans. Aerosp. Electron. Syst., April 2013, 49, (2), pp. 969–981. ISSN 0018-9251. doi:10.1109/TAES.2013.6494393

[27] Gatti, G., Falcone, M., Alpe, V., Malik, M., Burger, T., Rapisarda, M., Rooney, E.: 'GIOVE-B chilbolton in-orbit test: Initial results from the second galileo satellite'. Inside GNSS, September/October 2008, 3, (6), pp. 30–35

[28] Borio, D.: 'Squaring and cross-correlation codeless tracking: analysis and generalisation'. IET Radar, Sonar & Navigation, December 2011, 5, (9), pp. 958 –969

[29] Borio, D., Anantharamu, P., Lachapelle, G.: 'SATLSim: a semi-analytic framework for fast GNSS tracking loop simulations'. GPS Solutions, 2011, 15, pp. 427–431. ISSN 1080-5370

[30] Borio, D., Cano, E.: MATLAB - A Fundamental Tool for Scientific Computing and Engineering Applications - Volume 2, chapter 13, Semi-Analytic Techniques for Fast MATLAB Simulations. InTech 2012, pp. 285–310

[31] Galileo Project Office: GIOVE-A + B Navigation Signal-in-Space Interface Control Document. European Space Agency, ESTEC Keplerlaan 1 - 2201 AZ Noordwijk - The Netherlands, August 2008

[32] Borio, D., Rao, M., O'Driscoll, C.: 'Codeless processing of binary offset carrier modulated signals'. IET Radar, Sonar and Navigation, February 2013, 7, (2), pp. 143–152